An early lunar core dynamo driven by thermochemical mantle convection

Dave R. Stegman*, A. Mark Jellinek*†, Stephen A. Zatman‡§, John R. Baumgardner‖ & Mark A. Richards*

** Department of Earth and Planetary Science, University of California, Berkeley, California 94720, USA*
† Department of Physics, University of Toronto, Toronto, Canada M5S 1A7
‡ Department of Earth and Planetary Sciences, Washington University, St Louis, Missouri 63130, USA
‖ Theoretical Division, Los Alamos National Laboratory, Los Alamos, New Mexico 87545, USA
§ Deceased

Although the Moon currently has no internally generated magnetic field, palaeomagnetic data, combined with radiometric ages of Apollo samples, provide evidence for such a magnetic field from ~3.9 to 3.6 billion years (Gyr) ago[1], possibly owing to an ancient lunar dynamo[1,2]. But the presence of a lunar dynamo during this time period is difficult to explain[1–4], because thermal evolution models for the Moon[5] yield insufficient core heat flux to power a dynamo after ~4.2 Gyr ago. Here we show that a transient increase in core heat flux after an overturn of an initially stratified lunar mantle might explain the existence and timing of an early lunar dynamo. Using a three-dimensional spherical convection model[6], we show that a dense layer, enriched in radioactive elements (a 'thermal blanket'), at the base of the lunar mantle can initially prevent core cooling, thereby inhibiting core convection and magnetic field generation. Subsequent radioactive heating progressively increases the buoyancy of the thermal blanket, ultimately causing it to rise back into the mantle. The removal of the thermal blanket, proposed to explain the eruption of thorium- and titanium-rich lunar mare basalts[7], plausibly results in a core heat flux sufficient to power a short-lived lunar dynamo.

Table 1 **Model parameters**

Symbol	Description	Value
R_o	Radius of planet	1,740 km
R_i	Radius of core	450 km
L	Thickness of blanket layer	230 km
H	Depth of mantle	1,290 km
ρ_m	Density, mantle	3,400 kg m^{-3}
ρ_c	Density, core	7,400 kg m^{-3}
g_s	Gravity, surface of Moon	1.6 m s^{-2}
g_c	Gravity, surface of lunar core	0.93 m s^{-2}
α_m	Thermal expansivity, mantle	4×10^{-5} K^{-1}
α_c	Thermal expansivity, core	10^{-4} K^{-1}
k_m	Thermal conductivity, mantle	4 W m^{-1} K^{-1}
k_c	Thermal conductivity, core[30,31]	25–50 W m^{-1} K^{-1}
$c_{p,m}$	Heat capacity, mantle	1,400 J kg^{-1} K^{-1}
$c_{p,c}$	Heat capacity, core	850 J kg^{-1} K^{-1}
L_m	Latent heat, mantle	5×10^5 J kg^{-1}
T_o	Surface temperature	250 K
$T_c(t=0)$	Initial core temperature (models TB-0,1,2)	1,800 K
$T_s(0)$	Solidus temperature at surface, mantle	1,450 K
$T_s(P)$	Solidus temperature increase, mantle	0.1 K Mpa^{-1}
η_o	Reference viscosity, mantle	3×10^{20} Pa s
E	Activation energy	5×10^5 J mol^{-1}
V	Activation volume	1.5×10^{-6} m^3 mol^{-1}
a	Scaling for viscosity exponent	0.28
γ	Maximum viscosity variation	3,000
[U]	Uranium concentration	25.7 p.p.b.
Th/U	Thorium/uranium ratio	4
K/U	Potassium/uranium ratio	2,000
f	Fraction of radiogenic elements in mantle	0.25

$H(t)$ is heat production rate for bulk lunar mantle due to radioactive element concentrations listed above and their appropriate decay constants. Assuming that radiogenic elements are concentrated into the last 5% of mantle volume during magma ocean solidification, the heat production of the KREEP layer is $20H(t)$. During overturn, some fraction f of the KREEP layer is entrained into this downwelling flow and the resultant thermal blanket layer is assumed to have a uniform heat-production of $20fH(t)$.

Solidification of an early planetary-scale lunar magma ocean (see, for example, ref. 8) produced a chemically stratified mantle. An anorthosite crust was underlain by the last-solidified 'KREEP' (enriched in potassium, rare-earth elements and phosphorus) layer, containing most of the mantle's incompatible, radioactive heat-producing elements. Beneath the KREEP layer was an earlier-formed ilmenite cumulate[7] overlying a thick layer of pyroxenite, which formed the bulk of the lunar mantle. The proposed ilmenite cumulate layer is denser than the underlying pyroxenite[7]. Thus, shortly after solidification of the lunar mantle, the ilmenite cumulate layer overturned and sank into the mantle as a number of drips, ponding as a layer at the core–mantle boundary[9] (CMB). Some fraction of the KREEP layer must also have been viscously entrained into these downwellings. This dense, mixed ilmenite cumulate layer overlying the CMB would have contained a high concentration of radioactive elements. Subsequent radioactive decay and internal heating of this layer might have caused it to become thermally buoyant and rise back into the overlying mantle[7,10]. Without the downward transport of heat-producing elements provided by an initial overturn, a purely conductive model could reasonably describe the lunar thermal evolution[11].

We propose that the removal of this dense, internally heated layer (thermal blanket) overlying the core caused a transient increase in the core heat flux that was sufficient to power a lunar dynamo. However, to explain the observed palaeomagnetic intensity data, three criteria must be satisfied. First, the core cooling must be sufficiently rapid to drive thermal convection in the core[3,12–15]. Second, convective motions in the core must supply enough magnetic energy to power a strong-field dynamo[12–15], the regime in which terrestrial planetary magnetic fields are thought to be generated[16]. Third, this dynamo must produce magnetic field strengths at the lunar surface that are compatible with the palaeointensity data[1–3] (Fig. 1i).

Thermal convection inside a molten iron core occurs when the core heat flux exceeds that conducted down the core adiabat[12–15], $Q_{ad} = \alpha_c T_c k_c g_c / c_{p,c}$ (see Table 1 for symbol definitions and values). Although both the initial temperature and composition of the core are poorly constrained, the current presence of a fluid core[17] implies that the core is not pure iron but instead contains a low-density impurity such as sulphur, which has lowered its freezing temperature. The solidification of a pure-Fe inner core from a liquid Fe–S alloy probably began early in the evolution of the lunar core and drove compositional convection[13]. Gravitational potential energy supplied by compositional convection would increase, by as much

Table 2 **Model runs**

Case	Buoyancy number, B	Initial temperature drop across CMB, ΔT (K)
TB-0	0	200
TB-1	1.0	200
TB-2	0.5	200
TB-3	0.5	0

We use a massively parallel, finite element model (LUNA), adapted from TERRA[6,18,19], with a lagrangian particle tracer method[32] to accommodate the heterogeneous distribution of chemically dense material, a smaller core relative to the planet's radius (the temperature of which can evolve according to the conservation of heat at the core–mantle boundary) and time-dependent, heterogeneous heat production. The model also accounts for the conservation of latent heat on melting throughout the depth of the mantle. The computational mesh resolution is 10 km at the inner surface and 30 km at the outer surface and each element initially contains 10 particles, which carry chemical-density and heat-production information. The core radius is 450 km, which for technical reasons associated with the numerical grid employed is the smallest size currently possible but is just outside the range of observational constraints on lunar core size. Because mantle convection occurs beneath a 'stagnant lid'[20,21], we impose a no-slip boundary condition at the surface and a free-slip condition at the core–mantle boundary. The radial viscosity of lunar mantle depends on temperature according to $\eta(T) = \eta_0 e^{a[(E+PV)/RT]}$, where T is the laterally averaged temperature at each depth and a is a damping constant introduced for technical reasons that limits the exponential temperature dependence of viscosity[19]. Even with the more modest sensitivity to temperature in these models, there is still a viscosity variation in the calculations, γ (measured as the ratio of largest to smallest viscosities), equal to 3,000, most of which is in the upper thermal boundary layer. Ignoring lateral viscosity variations affects the detailed form of upwellings and downwellings but still allows us to capture the essential thermal evolution of the models, as well as the basic nature of the hot and cold thermal boundary layers[33]. The ΔT used in B is the temperature drop across the interface between ambient mantle and the thermal blanket layer, as determined in case TB-1 (ref. 24). The chosen B is only an initial value, because B evolves during the calculation.

as an order of magnitude, estimates for the energy available to drive a dynamo based on thermal convection alone[13,14]. However, this additional energy depends on the surface area of the inner core. Because both the sulphur concentration and initial temperature in the core are poorly constrained it is difficult to estimate the size of an early inner core. Thus, we are unable to assess the role of compositional convection. Our initial goal is, therefore, to identify conditions in which thermal evolution models predict thermal

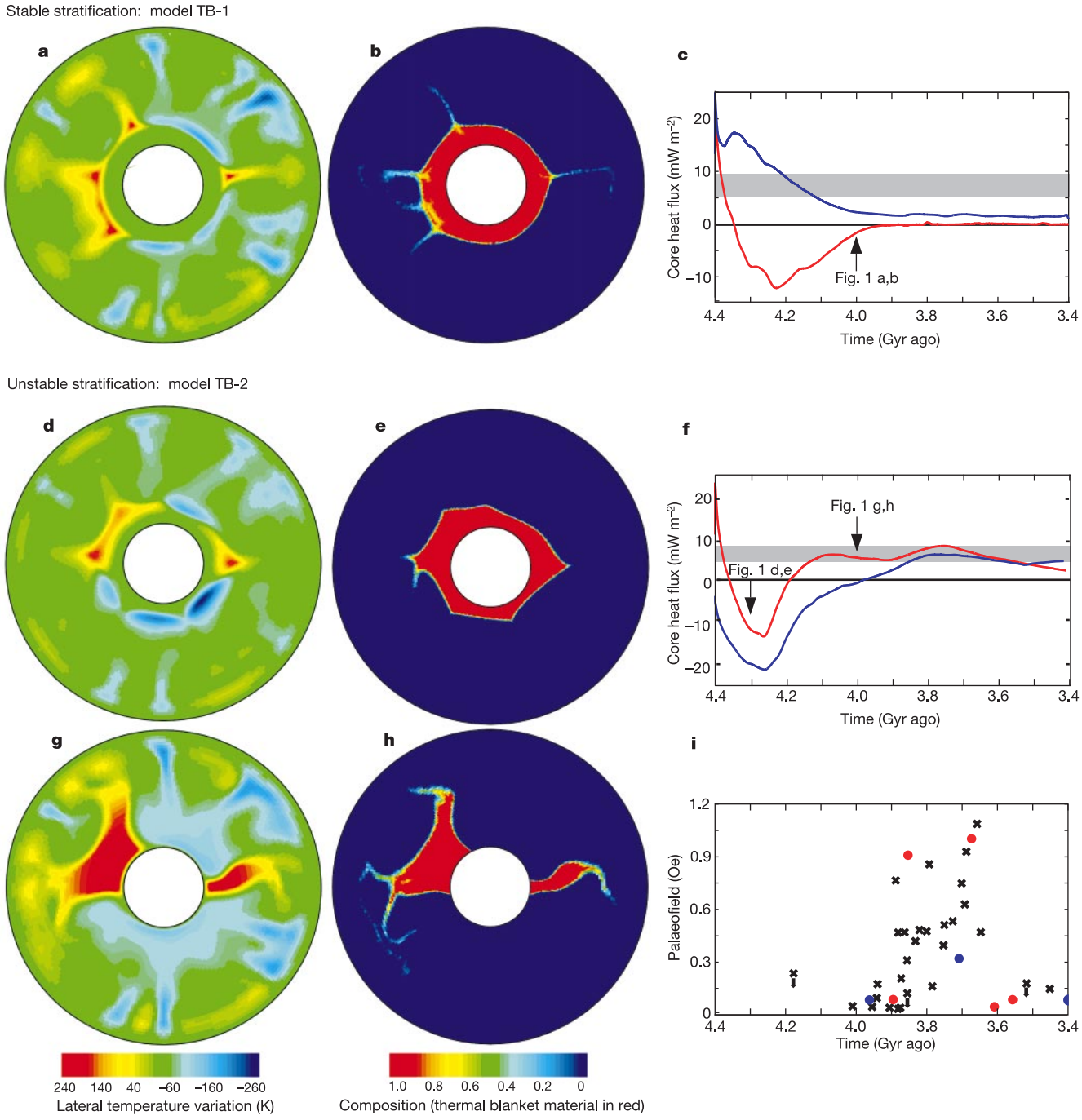

Figure 1 Thermochemical evolution models in stable (**a**–**c**) and unstable (**d**–**h**) thermal blanket regimes as seen in temperature (**a**, **d**, **g**), composition (**b**, **e**, **h**) and core heat flux (**c**, **f**) compared with palaeomagnetic intensity data (**i**). The equatorial cross-sections of temperature (**a**) and composition (**b**) for model TB-1 at 4.0 Gyr ago show that thermal blanket material is too dense to become buoyant, but some entrainment occurs. However, equatorial cross-sections of temperature and composition for model TB-2 show a marginally stable thermal blanket interacting with mantle convection at 4.3 Gyr ago (**d**, **e**) and that by 4.0 Gyr ago (**g**, **h**) has sufficient thermal buoyancy to rise back towards the lunar surface. **c**, The core thermal history for reference model TB-0 shows heat flux values (blue line) well below adiabatic core heat flux (grey region), whereas model TB-1 (red line) has nearly zero heat flux (black line). Such core heat flux values ranging between the black line and grey region indicates a thermally stratified core in which all core heat loss is by conduction and no dynamo is supported. **f**, Thermal blanket ($B = 0.5$). Red line, initial ΔT at CMB = 200 K; blue line, initial ΔT at CMB = 0 K. A core heat flux equal to or above the shaded region indicates core convection and the probable occurrence of a dynamo, as seen in models TB-2 and TB-3. **i**, Palaeointensity measurements from Apollo samples (modified from ref. 1) in which dots indicate absolute palaeointensity measurements (Thellier–Thellier method in red; other techniques in blue) and crosses indicate scaled normalized relative palaeointensities. In our models, asymmetric removal of the thermal blanket leads to a localized distribution of partly molten thermal-blanket material at relatively shallow mantle depths, confirming a plausible explanation for the eruption of high-thorium, high-titanium mare basalts, similar to the models in ref. 10. Our models make no attempt to evaluate melt transport to the surface. 1 Oe $\approx$ 79.6 A m^{-2}.

convection in the core (that is, $Q_{cmb} > Q_{ad}$).

Internal radioactive heating and cooling at the Moon's surface result in mantle convection. To model early lunar mantle convection, we use a three-dimensional spherical numerical model described in detail elsewhere[6,18,19]. Reasonable lunar mantle properties (Tables 1, 2) yield a Rayleigh number, $Ra = \rho g \alpha \Delta T H^3 / \mu \kappa = 3 \times 10^6$, appropriate for the early Moon. Because the lunar crust is thought to have remained intact from shortly after the Moon's formation, mantle convection has evidently occurred in the 'stagnant-lid' regime, in which large viscosity variations due to the temperature dependence of mantle viscosity results in an immobile upper thermal boundary layer, or lithosphere, and a thin sublayer subject to convective instability[20,21]. This sublayer has a viscosity that is about an order of magnitude larger than the underlying mantle[21], corresponding to a temperature difference of ~100 K. Such weak cooling, characteristic of stagnant-lid convection, leads to unfavourable conditions for dynamo generation[22].

Our models begin ~100 Myr after Moon formation, during which time solidification of the magma ocean occurs, dense material ponds at the base of the mantle, and solid-state mantle convection begins. Initially the dense layer is 230 km thick and has a uniform density indicated by the buoyancy number, $B = \Delta\rho_{chem} / \alpha_m \Delta T$. The temperature profile beneath the upper thermal boundary layer is that of the mantle solidus to 400 km depth. Below this depth, the temperature is taken to be a constant 1,600 K, similar to that in other studies[5,10]. We examine initial core temperatures 0–200 K hotter than the overlying mantle[5] (Table 2).

Model TB-0 is a reference thermal evolution case[5] in which the core cools to a mantle of uniform density and composition (no thermal blanket). Core temperatures range from 1,600 to 1,700 K, giving $Q_{ad} = 5.0$–$9.0\ mW\ m^{-2}$. Typical of one-plate planets, the core heat flux, Q (blue line in Fig. 1c), exceeds Q_{ad} (shaded region) only for the first few hundred million years, an effect of the core's beginning 200 K hotter than the mantle. Such simple thermal evolution models[5] fail to generate core convection after about ~4.2 Gyr ago.

In model TB-1 (Fig. 1a–c), $B = 1.0$ and the thermal blanket is stable[23,24]. The thermal blanket heats the outermost portion of the core (red line in Fig. 1c). At about 4 Gyr ago, several hot plumes rise from the top of the thermal blanket into the overlying mantle entraining small amounts of dense material. After ~4 Gyr ago, the core cools more slowly than for TB-0. $Q < Q_{ad}$ except in the very earliest stages of evolution (~4.4 Gyr ago).

In model TB-2, $B = 0.5$ and the thermal blanket is marginally stable[23,24]. Initially, as in model TB-1, the thermal blanket warms the lunar core (Fig. 1d and e). However, prolonged internal radioactive heating increases the buoyancy of the thermal blanket, so that it ultimately rises into overlying mantle as a few large upwelling plumes[10] (Fig. 1g and h). The removal of the thermal blanket causes $Q \geq Q_{ad}$ from ~4.0 to 3.5 Gyr ago, coincident with the magnetic era (~3.9 to 3.6 Gyr ago). Even in the case for which the core and lowermost mantle begin in thermal equilibrium, model TB-3 (blue line in Fig. 1f), evolves such that $Q \geq Q_{ad}$.

Our results show that all simple layered (TB-1) or unlayered (TB-0) models lead to core heat fluxes an order of magnitude too small to drive thermal convection in the core during the magnetic era. However, in the marginally stable regime[23,24] (TB-2), the removal of a thermal blanket owing to internal heating and dynamic coupling with mantle convection results in a core heat flux sufficient to drive thermal convection in the core for a few hundred million years beginning ~4 Gyr ago. Furthermore, a key prediction of model TB-2 is that a well-defined onset time for the lunar dynamo, approximately coincident with thermal blanket removal, might be observable ~4.2–3.9 Gyr ago (Fig. 1f).

Whether model TB-2 results in a strong-field dynamo[16] depends on the efficiency with which the available gravitational potential energy driving thermal convection is converted into magnetic energy through ohmic dissipation (see ref. 14, for example). For a core of radius of 350–450 km (refs 17, 25), ohmic dissipation must exceed ~30–70 MW to support the strong-field regime[14,16]. Applying the lunar core properties in Table 1 to the study of Buffett *et al.*[14] indicates that, during the period that model TB-2 has a superadiabatic core heat flux, the ohmic heat dissipation is ~0.1–0.2% of the total core heat flow. This efficiency implies that ~20–40 MW is available for ohmic dissipation and thus a strong-field dynamo is plausible. Additional forcing by compositional convection[13,14] would further increase the energy available to drive a dynamo.

The surface magnetic field strength resulting from model TB-2 is difficult to constrain. The magnetic field is partitioned into two components: a toroidal component that remains in the core and a poloidal component observable at the surface. The partitioning of magnetic field energy between these two components is unknown. However, poloidal magnetic field strength is proportional to $1/R^3$.If model TB-2 supports a 12-G (1 gauss = 10^4 tesla) core field (strong-field dynamo) by thermal convection alone, and the poloidal component represents about half of that, the maximum surface field strength would be ~0.1 G. To achieve even stronger surface fields (0.2–0.5 G), consistent with those observed during the magnetic era (Fig. 1i), core field strengths of 20–60 G are needed. This suggests compositional convection driven by the growth of an inner core was an important process during the magnetic era.

The results of model TB-2 might also explain the origin of the recently recognized Procellarum KREEP Terrane (PKT)[11,26,27], a province defined by its elevated levels of thorium, which has undergone extensive resurfacing by mare volcanism. Petrological analyses of volcanic glasses[28] support the inferences from remotely sensed data that high-thorium, high-titanium basalts exist within the PKT[27,29], although Apollo basalt samples from this region are low in thorium[11]. Moreover, the depths of origin of these glasses can exceed 500 km (refs 27–29) and might share a mantle source with PKT basalts. If the high-titanium source region originally solidified at a shallow depth (<100 km)[7,8], a cumulate overturn model[7,10] might account for such deep melting nearly 500 Myr later. Zhong *et al.*[10] reported that although the proposed overturn was a global event, the ilmenite cumulate material that had ponded at the CMB probably rose back to the surface asymmetrically, producing localized high-thorium, high-titanium volcanism. Our results are consistent with thermal blanket removal's being an inherently asymmetric process and thus provide a self-consistent explanation for both the existence of an ancient lunar dynamo as well as the origin, composition and duration of mare volcanism in the PKT. □

Received 25 June; accepted 25 October 2002; doi:10.1038/nature01267.

1. Cisowski, S. M., Collinson, D. W., Runcorn, S. K. & Stephenson, A. A review of lunar paleointensity data and implications for the origin of lunar magnetism. *J. Geophys. Res.* **88,** A691–A704 (1983).
2. Collinson, D. W. Magnetism of the Moon—A lunar core dynamo or impact magnetization? *Surv. Geophys.* **14,** 89–118 (1993).
3. Stevenson, D. J. Planetary magnetic fields. *Rep. Prog. Phys.* **46,** 555–620 (1983).
4. Runcorn, S. K. The formation of the lunar core. *Geochim. Cosmochim. Acta* **60,** 1205–1208 (1996).
5. Konrad, W. & Spohn, T. Thermal history of the Moon: Implications for an early core dynamo and post-accretional magmatism. *Adv. Space Res.* **19,** 1511–1521 (1997).
6. Baumgardner, J. R. Three dimensional treatment of convective flow in the Earth's mantle. *J. Stat. Phys.* **39,** 501–511 (1985).
7. Hess, P. C. & Parmentier, E. M. A model for the thermal and chemical evolution of the Moon's interior: Implications for the onset of mare volcanism. *Earth Planet. Sci. Lett.* **134,** 501–514 (1995).
8. Warren, P. H. The magma ocean concept and lunar evolution. *Annu. Rev. Earth Planet. Sci.* **13,** 201–240 (1985).
9. Jellinek, A. M., Kerr, R. C. & Griffiths, R. W. Mixing and compositional stratification produced by natural convection. 1. Experiments and their application to Earth's core and mantle. *J. Geophys. Res.* **104,** 7183–7202 (1999).
10. Zhong, S., Parmentier, E. M. & Zuber, M. T. A dynamic origin for the global asymmetry of lunar mare basalts. *Earth Planet. Sci. Lett.* **177,** 131–140 (2000).
11. Wieczorek, M. A. & Phillips, R. J. The 'Procellarum KREEP Terrane': Implications for mare volcanism and lunar evolution. *J. Geophys. Res.* **105,** 20417–20430 (2000).
12. Stevenson, D. J., Spohn, T. & Schubert, G. Magnetism and thermal evolution of the terrestrial planets. *Icarus* **54,** 466–489 (1983).
13. Stacey, F. D. & Loper, D. E. Thermal histories of the core and mantle. *Phys. Earth Planet. Inter.* **36,** 99–115 (1984).

14. Buffett, B. A., Huppert, H. E., Lister, J. R. & Woods, A. W. On the thermal evolution of the Earth's core. *J. Geophys. Res.* **101,** 7989–8006 (1996).
15. Stevenson, D. J. Mars' core and magnetism. *Nature* **412,** 214–219 (2001).
16. Roberts, P. H. & Soward, A. M. Dynamo theory. *Annu. Rev. Fluid Mech.* **24,** 459–512 (1992).
17. Williams, J. G., Boggs, D. H., Yoder, C. F. & Ratcliff, J. T. Lunar rotational dissipation in solid body and molten core. *J. Geophys. Res.* **106,** 27933–27968 (2001).
18. Bunge, H.-P. & Baumgardner, J. R. Mantle convection modeling on parallel virtual machines. *Comput. Phys.* **9,** 207–215 (1995).
19. Yang, W.-S. & Baumgardner, J. R. A matrix-dependent transfer multigrid method for strongly variable viscosity infinite Prandtl number thermal convection. *Geophys. Astrophys. Fluid* **92,** 151–195 (2000).
20. Christensen, U. R. Heat transport by variable viscosity convection and implications for the Earth's thermal evolution. *Phys. Earth Planet. Inter.* **35,** 264–282 (1984).
21. Moresi, L.-N. & Solomatov, V. S. Numerical investigation of 2D convection with extremely large viscosity variations. *Phys. Fluids* **7,** 2154–2162 (1995).
22. Jellinek, A. M., Lenardic, A. & Manga, M. The influence of interior mantle temperature on the structure of plumes: Heads for Venus, tails for Earth. *Geophys. Res. Lett.* **29,** doi:10.1029/2001GL014624 (2002).
23. Davaille, A. Simultaneous generation of hotspots and superswells by convection in a heterogeneous planetary mantle. *Nature* **402,** 756–760 (1999).
24. Gonnermann, H. M., Manga, M. & Jellinek, A. M. Dynamics and longevity of an initially stratified mantle. *Geophys. Res. Lett.* **29,** doi:10.1029/2002GL01485 (2002).
25. Hood, L. L., Mitchell, D. L., Lin, R. P., Acuna, M. H. & Binder, A. B. Initial measurements of the lunar induced magnetic dipole moment using Lunar Prospector magnetometer data. *Geophys. Res. Lett.* **26,** 2327–2330 (1999).
26. Jolliff, B. L., Gillis, J. J., Haskin, L. A., Korotev, R. L. & Wieczorek, M. A. Major lunar crustal terranes: Surface expressions and crust–mantle origins. *J. Geophys. Res.* **105,** 4197–4216 (2000).
27. Haskin, L. A., Gillis, J. J., Korotev, R. L. & Jolliff, B. L. The materials of the lunar Procellarum KREEP Terrane: A synthesis of data from geomorphological mapping, remote sensing, and sample analyses. *J. Geophys. Res.* **105,** 20403–20415 (2000).
28. Delano, J. Pristine lunar glasses: Criteria, data and implications. *J. Geophys. Res.* **91,** 201–213 (1986).
29. Hess, P. C. On the source regions for mare picrite glasses. *J. Geophys. Res.* **105,** 4347–4360 (2000).
30. Anderson, O. L. The Gruneisen parameter for iron at outer core conditions and the resulting conductive heat and power in the core. *Phys. Earth Planet. Inter.* **109,** 179–197 (1998).
31. Stacey, F. D. & Anderson, O. L. Electrical and thermal conductivities of Fe-Ni-Si alloy under core conditions. *Phys. Earth Planet. Inter.* **124,** 153–162 (2001).
32. Stegman, D. R., Richards, M. A. & Baumgardner, J. R. Effects of depth dependent viscosity and plate motions on maintaining a relatively uniform MORB reservoir in whole mantle flow. *J. Geophys. Res.* **107,** doi:10.1029/2001JB000192 (2002).
33. Tackley, P. J. Effects of strongly variable viscosity on 3-dimensional mantle convection. *J. Geophys. Res.* **101,** 3311–3332 (1996).

Acknowledgements We thank B. Buffett for helpful discussions; C. Johnson, R. Jeanloz, M. Manga and H.-P. Bunge for comments; and D. Stevenson and M. Zuber for reviews that improved this manuscript. We dedicate this work to the memory of our co-author Stephen Zatman, who inspired us by his interest in this subject. This work was supported by IGPP LANL, NASA CT project, the National Science Foundation, and the Miller Institute for Basic Research in Science.

Competing interests statement The authors declare that they have no competing financial interests.

Correspondence and requests for materials should be addressed to D.S. (e-mail: dstegman@eps.berkeley.edu).

Measuring intense rotation and dissipation in turbulent flows

Benjamin W. Zeff*, Daniel D. Lanterman*, Ryan McAllister*, Rajarshi Roy*, Eric J. Kostelich† & Daniel P. Lathrop*

* *Department of Physics, IPST and IREAP, University of Maryland, College Park, Maryland 20742-4111, USA*
† *Department of Mathematics, Arizona State University, Tempe, Arizona 85287-1804, USA*

Turbulent flows are highly intermittent—for example, they exhibit intense bursts of vorticity and strain. Kolmogorov theory[1,2] describes such behaviour in the form of energy cascades from large to small spatial and temporal scales, where energy is dissipated as heat. But the causes of high intermittency in turbulence, which show non-gaussian statistics[3–5], are not well understood. Such intermittency can be important, for example, for enhancing the mixing of chemicals[6,7], by producing sharp drops in local pressure that can induce cavitation (damaging mechanical components and biological organisms)[8], and by causing intense vortices in atmospheric flows. Here we present observations of the three components of velocity and all nine velocity gradients within a small volume, which allow us to determine simultaneously the dissipation (a measure of strain) and enstrophy (a measure of rotational energy) of a turbulent flow. Combining the statistics of all measurements and the evolution of individual bursts, we find that a typical sequence for intense events begins with rapid strain growth, followed by rising vorticity and a final sudden decline in stretching. We suggest two mechanisms which can produce these characteristics, depending whether they are due to the advection of coherent structures through our observed volume or caused locally.

The problem of turbulence has been notoriously difficult to resolve, because it involves the interaction of flow length and timescales over many orders of magnitude. The intense, localized events that are characteristic of turbulence can cause difficulty in numerical simulations, via the generation of small scales and large local gradients. Simulations have some advantage in that they provide access to the entire field; alternatively, experiments can yield long observational records that are computationally impractical. Turbulence experiments also have limitations. Many measurements have relied on invasive techniques[9] that can affect the flow being studied. Usually, measurements do not capture the full three-dimensional nature of the flow; instead, they rely on one- or two-component approximations of velocities and velocity gradients. A fully three-dimensional (3D), spatially resolved technique is needed to measure important quantities such as the energy dissipation and helicity within the flow. Good temporal resolution is also required to study the rapid development of intense events.

A few recent experiments have captured many of these features. Tao *et al.*[10,11] used holographic particle image velocimetry (HPIV) to take elegant 3D snapshots of turbulent channel flow, though the technique is not time-resolved. Using two very different technologies, La Porta *et al.*[12] and Mordant *et al.*[13] tracked individual particles (a lagrangian measurement) in highly turbulent flows. This

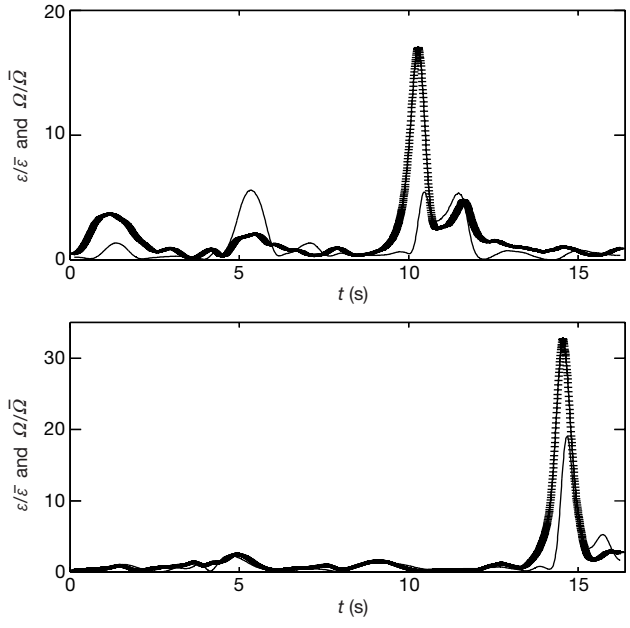

Figure 1 Time traces of the dissipation ε and enstrophy Ω. The two traces above show intense events occurring in a turbulent flow. Dissipation curves are marked with crosses, and enstrophy curves are shown as continuous curves. The time averages are $\bar{\varepsilon} = 0.0336\,\mathrm{cm^2\,s^{-3}}$ and $\bar{\Omega} = 4.13\,\mathrm{s^{-2}}$ with intermittent bursts reaching up to 40 times those values.

